

# UC Berkeley

## UC Berkeley Previously Published Works

### Title

Growth Factor Identity Is Encoded by Discrete Coiled-Coil Rotamers in the EGFR Juxtamembrane Region

### Permalink

<https://escholarship.org/uc/item/15x8r205>

### Journal

Cell Chemical Biology, 22(6)

### ISSN

2451-9456

### Authors

Doerner, Amy  
Scheck, Rebecca  
Schepartz, Alanna

### Publication Date

2015-06-01

### DOI

10.1016/j.chembiol.2015.05.008

Peer reviewed



# HHS Public Access

Author manuscript

*Chem Biol.* Author manuscript; available in PMC 2016 June 18.

Published in final edited form as:

*Chem Biol.* 2015 June 18; 22(6): 776–784. doi:10.1016/j.chembiol.2015.05.008.

## Growth factor identity is encoded by discrete coiled coil rotamers in the EGFR juxtamembrane region

Amy Doerner,

Department of Chemistry, Yale University, New Haven, Connecticut 06520-8107

Rebecca Scheck, and

Department of Chemistry, Yale University, New Haven, Connecticut 06520-8107

Alanna Schepartz

Department of Chemistry, Department of Molecular, Cellular and Developmental Biology, Yale University, New Haven, Connecticut 06520-8107

### Summary

Binding of the growth factor TGF- $\alpha$  to the EGFR extracellular domain is encoded through the formation of a unique anti-parallel coiled coil within the juxtamembrane segment. This new coiled coil is an ‘inside-out’ version of the coiled coil formed in the presence of EGF. A third, intermediary coiled coil interface is formed in the juxtamembrane segment when EGFR is stimulated with betacellulin. The seven growth factors that activate EGFR in mammalian systems (EGF, TGF- $\alpha$ , epigen, epiregulin, betacellulin, heparin-binding EGF, and amphiregulin) fall into distinct categories in which the structure of the coiled coil induced within the juxtamembrane segment correlates with cell state. The observation that coiled coil state tracks with the downstream signaling profiles for each ligand provides evidence for growth factor functional selectivity by EGFR. Encoding growth factor identity in alternative coiled coil rotamers provides a simple and elegant method for communicating chemical information across the plasma membrane.

### INTRODUCTION

There remains an incomplete understanding of how EGFR, the prototypic member of the receptor tyrosine kinase superfamily, communicates ligand identity across the plasma membrane. Despite multiple high-resolution views of the extracellular ligand-binding (Ferguson et al., 2003; Garrett et al., 2002; Ogiso et al., 2002) and intracellular kinase (Jura

**Contact information:** Alanna Schepartz, Department of Chemistry, Yale University, 225 Prospect St., New Haven CT 06520-8107. Phone: 203-432-5094; Fax: 203-432-3486; alanna.schepartz@yale.edu.

**Publisher's Disclaimer:** This is a PDF file of an unedited manuscript that has been accepted for publication. As a service to our customers we are providing this early version of the manuscript. The manuscript will undergo copyediting, typesetting, and review of the resulting proof before it is published in its final citable form. Please note that during the production process errors may be discovered which could affect the content, and all legal disclaimers that apply to the journal pertain.

#### SUPPLEMENTAL INFORMATION

Supplemental Information contains 5 figures and Supplemental Experimental Procedures and can be found with this article online at [add link].

#### AUTHOR CONTRIBUTIONS

A.D., R.S., and A.S. designed research; A.D. and R.S. performed research; A.D., R.S., and A.S. analyzed data; and A.D., R.S., and A.S. wrote the paper.

et al., 2009a; Zhang et al., 2006) domains and a rudimentary understanding of the basic activation mechanism (Arkhipov et al., 2013; Endres et al., 2013; Lu et al., 2010), how this information is decoded into ligand-dependent differences in cell state remains unclear (Wilson et al., 2009). In previous work, we made use of bipartite tetracysteine display (Luedtke et al., 2007) and the bis-arsenical dye ReAsH (Adams et al., 2002) to probe how ligand binding to the EGFR extracellular domain influences structure within the cytoplasmic juxtamembrane segment (Figure 1A). The juxtamembrane segment (JM) is a short (37 aa) sequence that links the extracellular ligand binding and transmembrane domains to the intracellular kinase domain and stabilizes the receptor active state (Jura et al., 2009a). We discovered that binding of the growth factor EGF to the EGFR extracellular domain induced the formation of a discrete anti-parallel coiled coil (Jura et al., 2009a) within the juxtamembrane-A (JM-A) segment, whereas binding of the alternative growth factor TGF- $\alpha$  induced an alternative, helical interface whose structure was not established (Figure 1A) (Scheck et al., 2012). As predicted by NOE's seen in short peptide models (Jura et al., 2009a), the EGF-induced antiparallel structure is characterized by leucine residues at the *a* and *d* positions of the paired heptad repeat and complementary electrostatic interactions at positions *e* and *g* (Figure S1B). Here we provide evidence that the helical interface formed in the presence of TGF- $\alpha$  is an 'inside-out' version of the EGF-induced structure, in which paired polar interactions predominate at the antiparallel interface (Figure S1C). We show further that the seven growth factors that activate EGFR in mammalian systems (EGF, TGF- $\alpha$ , epigen (EPI), epiregulin (ER), betacellulin (BC), heparin-binding EGF (HB), and amphiregulin (AR)) fall into distinct categories in which the structure of the coiled coil induced within the juxtamembrane segment correlates directly with cell state.

In our prior work, we designed three Cys-Cys EGFR variants (CC<sub>H</sub>-1, -2, and -3) (Figures 1B and S1A) that reported on the formation of the EGF-induced antiparallel coiled coil in live cells (Scheck et al., 2012). When this structure forms within a receptor dimer, the assembled tetracysteine motif is poised to bind ReAsH and cause it to fluoresce. Expression of CC<sub>H</sub>-1, -2, or -3 on the CHO-K1 cell surface resulted in a significant increase in normalized ReAsH fluorescence in the presence of EGF but not TGF- $\alpha$ . In contrast, expression of the EGFR variants CC<sub>H</sub>-5 and CC<sub>H</sub>-6 resulted in a significant increase in normalized ReAsH fluorescence in the presence of TGF- $\alpha$ , but not EGF (Scheck et al., 2012). Given the spatial requirements for ReAsH binding (Goodman et al., 2009), these observations led to the conclusion EGFR communicates ligand identity to the cytosol through at least two, discrete, helical JM-A conformations. Here we apply both computation and experiment to demonstrate that the helical interface formed in the presence of TGF- $\alpha$  is best characterized as an 'inside-out' version of the interface formed in the presence of EGF; the two antiparallel coiled coils are related by a 150° disrotatory rotation about each helix axis. We also identify a third, intermediary interface formed when EGFR is stimulated with betacellulin. We show further that the seven growth factors that activate EGFR in mammalian systems (EGF, TGF- $\alpha$ , epigen, epiregulin, betacellulin, heparin-binding EGF, and amphiregulin) fall into distinct categories in which the structure of the antiparallel coiled coil induced within the juxtamembrane segment correlates with downstream signaling outcomes. The observation that coiled coil state tracks with the downstream signaling profile for each ligand provides evidence for growth factor functional selectivity by EGFR.

Encoding growth factor identity in alternative coiled coil rotamers provides a simple and elegant method for communicating chemical information across the plasma membrane.

## RESULTS

### Evaluating the diversity of the JM helical landscape in silico

We first sought to identify the structure of the JM-A helical interface formed when EGFR is stimulated with TGF- $\alpha$ . Preliminary disulfide exchange and circular dichroism spectroscopy experiments revealed that peptides containing the minimal JM-A segment (residues 650 to 666) do not appreciably form dimers at concentrations below 150  $\mu$ M (Scheck et al., 2012; Sinclair et al., 2014) precluding a straightforward biophysical analysis of the isolated peptides. Thus, we turned to an *in silico* analysis to explore the diversity of the JM-A conformational landscape in the absence of complicating oligomerization events and then used bipartite tetracysteine display to detect these diverse conformations in the context of the intact receptor.

We used RosettaDock (Gray et al., 2003) to analyze thousands of potential dimeric JM-A helical interactions *in silico*. The interacting JM-A helices (residues 650–666) were oriented randomly, docked as rigid bodies, and the complexes subject to an all-atom minimization to optimize side chain conformations (Figure 2A). We generated 25,000 output structures, and the top-scoring 1,000 were clustered on the basis of RMSD differences. The 60 lowest-energy clusters–320 structures, roughly 1.3% of the total search space–were filtered to identify 15 clusters possessing the symmetric interface (homodimeric) that is prerequisite for ReAsH binding.

The 15 homodimeric clusters (Figure 2B) were highly diverse. As expected, the antiparallel structure for EGF-activated EGFR that was proposed by Jura et al. (Jura et al., 2009a) and confirmed by bipartite display (Scheck et al., 2012) and NMR (Endres et al., 2013; Jura et al., 2009a) defined one low energy cluster (antiparallel cluster 5) (Figure 2B and Figure S4D). However, the set of lowest-energy homodimeric clusters also contained many other structures whose helices were either parallel (36%) or antiparallel with significant deviation from cluster 5 (64%). The diversity of structures within an isolated but dimeric JM-A region predicted by RosettaDock is consistent with the short length (14 aa) of the interacting JM-A helices, which lack the compounding and biasing interactions provided by the intact, dimeric, receptor in complex with a specific activating growth factor. We turned to bipartite tetracysteine display to differentiate between these predicted models for full length EGFR on the cell surface.

### Evaluation of clusters containing parallel helices

We noticed that one cluster containing parallel homodimeric helices exhibited a favorable Rosetta Rank (parallel cluster 57). Closer examination indicated that the structures in this cluster (Figures S3A and S3B) possessed a leucine-rich helical interface much like the EGF-induced anti-parallel coil (Jura et al., 2009a) observed in cells (Scheck et al., 2012). This parallel structure would have assembled a favorable tetracysteine binding site for ReAsH within the JM-A of the CC<sub>H</sub>-1 EGFR dimer, as the Cys-Cys motif in each monomer lies

near the center of the JM-A sequence (Figure S1A, Figure S3C). As a result, CC<sub>H</sub>-1 alone cannot distinguish between the more frequently considered antiparallel structures in cluster 5 or the parallel structures found in cluster 57. Although the Cys-Cys motifs in CC<sub>H</sub>-2 and CC<sub>H</sub>-3 form non-ideal ReAsH binding sites in the structures found in cluster 57, this cluster could not be ruled out without additional experimentation, as only a slight helical rotation would be required to create an ideal ReAsH binding site. Thus, we sought to determine whether the parallel helical structures in cluster 57 are populated when full length EGFR is activated with EGF on the surface of live cells.

To identify the cluster 57 structures and distinguish them from the antiparallel structures in cluster 5, we designed a new EGFR variant suitable for bipartite tetracysteine display, CC<sub>H</sub>-7. This variant carries a Cys-Cys motif at the N-terminus of the JM-A sequence to ensure formation of a competent ReAsH binding site only if the parallel helical array in cluster 57 were to form (Figures S3E and S3F). Although CC<sub>H</sub>-7 expressed in CHO-K1 cells is active upon treatment with EGF (Figures S3G and S3H), ReAsH treatment did not result in a significant increase in fluorescence above background (Figures S3I and S3J). The same result was observed when cells expressing CC<sub>H</sub>-7 were treated with TGF- $\alpha$ . These observations failed to provide evidence for formation of the parallel coiled coil in cluster 57 when EGFR is activated with EGF (Scheck et al., 2012).

Having validated the utility of RosettaDock to refine our understanding of the EGF-induced structure within the EGFR JM-A dimer, we next sought to identify the most likely structure formed when EGFR is instead activated by TGF- $\alpha$ . We turned first to one set of related, parallel coiled coils (parallel cluster 53, Figures S3A and S3B) that would support ReAsH binding by the two previously reported EGFR variants CC<sub>H</sub>-5 and CC<sub>H</sub>-6 (Figures 1B and S3D), and thus, could represent the alternative TGF- $\alpha$ -induced conformation(s). To test for this parallel structure using bipartite tetracysteine display, we designed EGFR variant CC<sub>H</sub>-8, using the same strategy used to design CC<sub>H</sub>-7, with cysteine residues at the C-terminus of the helical interaction (Figures S3E and S3F). As was found for experiments employing CC<sub>H</sub>-7, while CC<sub>H</sub>-8 expressed in CHO-K1 cells is active upon treatment with TGF- $\alpha$  (Figures S3G and S3H), treatment with ReAsH led to no significant increase in fluorescence above background (Figures S3I and J). Taken together, the *in silico* and bipartite display experiments described suggest that neither EGF nor TGF- $\alpha$  induce the formation of a parallel helical interface within activated EGFR.

### Evaluation of clusters containing antiparallel helices

Having ruled out the parallel structure clusters we next considered the large number of low energy antiparallel structure clusters identified by RosettaDock to determine if any could be populated when EGFR is activated with TGF- $\alpha$ . We focused on two clusters whose antiparallel structures were both low energy and compatible with the previously observed ReAsH binding to EGFR variants CC<sub>H</sub>-5 and/or CC<sub>H</sub>-6 upon TGF- $\alpha$  activation (Figures 1B and S1A): clusters 1 and 49 (Figures 2B, 3A, and S4D) (Scheck et al., 2012). Antiparallel cluster 1 contains lower energy structures, but the structures in antiparallel cluster 49 form better ReAsH binding sites with the CC<sub>H</sub>-5 and CC<sub>H</sub>-6 Cys-Cys motifs (Figure S4A). We

thus turned to bipartite tetracysteine display to differentiate between these models for TGF- $\alpha$ -activated EGFR expressed on the mammalian cell surface.

Differentiating between the structures in clusters 1 and 49 using ReAsH and bipartite tetracysteine display required careful design. This design recognizes that ReAsH binding sites on antiparallel coiled coils fall into three categories (Figure 4). Antiparallel arrays with Cys-Cys motifs at positions *a* and *d*; *g* and *d*; or *a* and *e* within a single heptad repeat (shown in green) support robust ReAsH binding and fluorescence, whereas those with Cys-Cys motifs at positions *f* and *c* and *f* and *b* (shown in red) do not. More context dependent are sites in the third category, antiparallel arrays carrying Cys-Cys motifs at positions *b* and *e* or *c* and *g* (shown in gray)—these structures could support ReAsH binding and fluorescence in the context of a flexible JM structure. With these guidelines, we designed CC<sub>H</sub>-9 to differentiate between the structures in clusters 1 and 49 (Figure 3B). In this EGFR variant, the Cys-Cys motif occupies the favorable *g* and *d* (and *g'* and *d'*) positions if the helices are arranged as prescribed by cluster 1, and the unfavorable *f* and *c* (and *f'* and *c'*) positions if the helices are arranged as prescribed by cluster 49 (Figure S4B). Thus, TGF- $\alpha$ -treated cells expressing CC<sub>H</sub>-9 should fluoresce after ReAsH treatment if a cluster 1 coiled coil is formed within the EGFR JM-A, but not if a cluster 49 coiled coil has formed.

#### Evidence that the TGF- $\alpha$ -induced coiled coil is 'inside-out'

Examination of cells transfected with CC<sub>H</sub>-9 (Figure 3C) revealed that addition of TGF- $\alpha$  led to a greater than 2-fold increase in ReAsH fluorescence in comparison to untreated CC<sub>H</sub>-9-expressing cells, favoring cluster 1 as the JM-A structure formed in the presence of TGF- $\alpha$  and ruling out cluster 49 (Figure 3D). Nevertheless, we observed that cells transfected with CC<sub>H</sub>-9 also exhibited a 1.5-fold increase in ReAsH fluorescence in the presence of EGF, presumably because when the EGF-type coiled coil is formed (cluster 5), the Cys-Cys motif in CC<sub>H</sub>-9 occupies the ambiguous *b* and *e* positions (Figure S4B). As we desired an EGFR variant that would bind ReAsH and fluoresce only when activated with TGF- $\alpha$ , we next designed CC<sub>H</sub>-10 (Figure 3B). Here, the Cys-Cys motif occupies the favorable *a* and *d* (and *a'* and *d'*) positions if the helices are arranged as prescribed by cluster 1 (induced by TGF- $\alpha$ ) and the unfavorable *b* and *f* (and *b'* and *f'*) positions if the helices are arranged as prescribed by cluster 5 (induced by EGF) (Figure S4C). As a result, we would expect that cells expressing CC<sub>H</sub>-10 should fluoresce after ReAsH treatment when a cluster 1 structure is present, but not when a cluster 5 coiled coil has formed; therefore, these cells should fluoresce only in the presence of TGF- $\alpha$ . Western blot analysis of cells transfected with CC<sub>H</sub>-10, WT EGFR and CC<sub>H</sub>-1 showed similar patterns of C-terminal phosphorylation (Figures S4E and S4F); TIRF microscopy (Figure 3E) revealed that addition of TGF- $\alpha$  to cells transfected with CC<sub>H</sub>-10 led to a 1.5-fold increase in ReAsH fluorescence whereas addition of EGF had no effect (Figure 3F). Taken together, the observation of robust ReAsH fluorescence when cells expressing either CC<sub>H</sub>-9 or CC<sub>H</sub>-10 are treated with TGF- $\alpha$ -provides compelling evidence that the antiparallel helical structures in cluster 1 best represent the JM when EGFR is activated by TGF- $\alpha$ . Moreover, the EGFR variant CC<sub>H</sub>-10 can specifically detect this conformation and distinguish it from the EGF-activated state embodied by cluster 5.

### Coiled coil structure correlates with effect on cell state

Seven growth factors activate EGFR, five in addition to EGF and TGF- $\alpha$ : epigen (EPI), epiregulin (ER), betacellulin (BC), heparin-binding EGF (AB), and amphiregulin (AR). Numerous studies have shown that these seven growth factors segregate into two categories when their effects on downstream signaling are compared: activation with EGF, HB, or BC leads to greater receptor down-regulation and a shorter signaling pulse, while activation with TGF- $\alpha$ , AR, ER, or EPI promote receptor recycling and sustained signaling that increases cell proliferation (Baldys et al., 2009; Ebner and Derynck, 1991; Reddy et al., 1998; Roepstorff et al., 2009; Seth et al., 1999; Thoresen et al., 1998; Wilson et al., 2012). As ligand identity must be translated through the receptor to intracellular signaling proteins, we sought to determine—using CC<sub>H</sub>-1 and CC<sub>H</sub>-10—whether these signaling differences correlated with JM-A conformation. To evaluate the presence of the EGF-type coiled coil (represented by cluster 5) or the TGF- $\alpha$ -type coiled coil (represented by cluster 1), we treated cells expressing the EGFR variants CC<sub>H</sub>-1 or CC<sub>H</sub>-10 with saturating concentrations (as determined by Western blot, see Figures S5A and S5H) of AR, BC, ER, EPI, and HB and monitored ReAsH fluorescence (Figures 5A and S5B). Examination of cells transfected with CC<sub>H</sub>-1 revealed a 2-fold increase in ReAsH fluorescence upon addition of BC, HB, and EGF, but not upon addition of TGF- $\alpha$ , AR, ER, or EPI. By contrast, cells transfected with CC<sub>H</sub>-10 displayed a 1.5-fold increase in ReAsH fluorescence upon addition of TGF- $\alpha$ , AR, and ER and a 1.3-fold increase for BC and EPI but no increase in ReAsH fluorescence was observed upon addition of HB and EGF (Figure 5A). We attribute the lower fold increase upon EPI treatment to lower ligand potency, as detected by EGFR autophosphorylation (Figures S5A and S5H). Thus, with the exception of betacellulin (BC) (vide infra), there is a direct correlation between the effect of a growth factor on JM-A structure and the temporal dynamics of the overall signaling response.

### A third JM conformation is formed upon BC activation

Among the growth factors that activate EGFR, BC is unique in its ability to elicit robust ReAsH fluorescence from cells expressing either CC<sub>H</sub>-1 or CC<sub>H</sub>-10 (Figure 5A). This observation suggests that BC either induces both the TGF- $\alpha$ - and EGF-type coiled coils, presumably due to a significant increase in flexibility, or that it induces a third, intermediary conformation that is compatible with ReAsH binding by both CC<sub>H</sub>-1 and CC<sub>H</sub>-10. To distinguish these possibilities, we returned to the top-scoring structure clusters predicted by RosettaDock (Figure 2B). Because BC activation led to robust ReAsH fluorescence in both CC<sub>H</sub>-1 and CC<sub>H</sub>-10-expressing cells, we looked to identify structures that positioned the Cys-Cys motifs in both CC<sub>H</sub>-1 and CC<sub>H</sub>-10 such that ReAsH fluorescence could be observed using either variant (Figure 4). This strategy identified three possible models: those in clusters 12, 55, and 49 (Figures 5B and S5E) (see Figure S5C for Cys-Cys motif placements in each model).

To differentiate between these three models, we turned to previously designed EGFR variants. First, we predicted that CC<sub>H</sub>-9 should provide a robust ReAsH binding site if the JM-A 248 were to assemble into structures in cluster 12 or 55, but a poor site if it assembled into structures from cluster 49 (Figure S5D). Treatment of CC<sub>H</sub>-9-expressing cells with BC led to a two250 fold increase in ReAsH fluorescence relative to untreated cells (Figures



5D and S5G). The in251 crease in ReAsH fluorescence observed in this case effectively rules out the formation of cluster 49 structures in the presence of BC, but fails to differentiate between the structures represented by clusters 12 and 55. Thus, we turned to CC<sub>H</sub>-5, which would generate a poor ReAsH-binding site if the JM-A is assembled as prescribed by cluster 12, and an ambiguous site if assembled as prescribed by cluster 55. Treatment of CC<sub>H</sub>-5-expressing cells with BC did not result in a significant increase in ReAsH fluorescence relative to untreated cells (Figures 5D and S5G). The fact that CC<sub>H</sub>-5 does not bind ReAsH upon activation by BC supports the model represented by cluster 12, which was predicted to display a poor site for ReAsH binding with the CC<sub>H</sub>-5 Cys- Cys motifs (Figure S5D). Together these results suggest that activation by BC does not simply increase the flexibility of the JM-A, but rather leads to the formation of a discrete helical interface that is represented by the structures in cluster 12.

## DISCUSSION

The TGF- $\alpha$ -type antiparallel coiled coil induced in the JM-A by TGF- $\alpha$ , AR, EPI and ER and identified by tetracysteine bipartite display differs in unmistakable ways from the EGF-type structure identified previously (Figure 5E) (Jura et al., 2009a). With TGF- $\alpha$  bound, the two JM-A helices are rotated by 150° in opposite directions about the helical axis relative to the EGF-bound structure. This disrotatory motion flips the coiled coil inside-out, effectively interchanging those residues at the coiled coil interface for those on the outside surface. In contrast to the coiled coil interface induced by EGF, which is stabilized by leucines at the *a* and *d* positions and complementary salt bridge interactions at positions *e* and *g*, the TGF- $\alpha$ -type interface contains polar residues at these positions and leucine residues on the coiled coil exterior (Figures S1B and S1C). In particular, our data point to a TGF- $\alpha$ -induced antiparallel structure stabilized by salt bridge/polar interactions between R657 (at position *a*) and R656 (at position *g*) on one helix and E'661 (at position *e'*) and Q'660 (at position *d'*), respectively, on the other. The JM-A conformation induced when EGFR is activated by betacellulin (BC), represented by cluster 12, is intermediate between the EGF- and TGF- $\alpha$ -activated structures, possessing both a hydrophobic and polar interface. Specifically, the BC-type coiled coil utilizes a leucine interface at the *d* and *g* (and *d'* and *g'*) positions while using complementary polar interactions between R656 and Q660 at the *a* and *e* (and *a'* and *e'*) positions. It has been hypothesized that the residues on the outside of the short coiled coil could interact with the membrane (Endres et al., 2013; Jura et al., 2009i). While we chose to examine the unbiased interaction between the two JM-A helices, we did observe positively charged residues on the outside of the EGF-activated (R653 and R657), TGF- $\alpha$ -activated (K652 and R662) and BC-activated (R651, R657, and R662) conformations, further validating these models in the context of the whole, membrane-embedded receptor.

We note that while coiled coil interfaces in natural proteins are often stabilized by hydrophobic interactions, there has been a more recent appreciation of stabilizing polar salt bridges (Meier et al., 2010). In fact, among dimeric, antiparallel polar coiled coil interfaces, the most common interfacial motif consists of polar residues at the core positions *gd'*, *dg'*, *ae'*, and *ea'*—precisely the arrangement seen in TGF- $\alpha$ -cluster 1 (Meier et al., 2010). Coiled coils stabilized by polar interactions have been observed in proteins whose function demands multiple interhelical interfaces (Croasdale et al., 2011) and short sequences that



facilitate dimerization (Burkhard et al., 2000), two characteristics shared with the EGFR JM. Thus, the JM-A sequence, which possesses residues for both a hydrophobic helical interface and multiple salt bridging residues, uniquely allows the receptor to adopt multiple, distinct conformations.

In this work, we correlate previously identified ligand-dictated, downstream signaling differences to induced structure within the JM: a more down-regulated, shorter signaling pulse upon EGF and HB-EGF activation is associated with formation of a JM-A conformation in which leucine residues mediate the interhelical interface. On the other hand, the more recycled receptor with a sustained signaling pulse that results from TGF- $\alpha$ , AR, ER, and EPI activation is associated with formation of an “inside-out” JM-A conformation in which polar interactions line the interface and hydrophobic leucine residues are on the outside. The correlation breaks down for a single outlier—betacellulin (BC)—whose activated JM-A conformation is intermediary with only a 50 degree disrotatory motion separating the two. It is possible that these two structures are close enough to induce similar signaling downstream of the receptor, or perhaps the difference in helical structure has an impact on signaling outcomes that are presently not appreciated (Saito et al., 2004). It has been posited that receptor flexibility is an intrinsic property of receptors capable of engaging multiple ligands and signaling proteins (Nygaard et al., 2013), potentially explaining why this molecular mechanism has been difficult to study in many receptor tyrosine kinases.

The ligand-dependent differences in JM structure uncovered in this work imply analogous ligand-dependent differences in the conformation of the bound ECD that are propagated to the JM through domain IV and the TM domain. We have previously shown that differences in the binding modes of EGF and TGF- $\alpha$  must lead to differential positioning of domain IV in the ECD (Scheck et al., 2012). In addition, MD simulations have revealed subtle differences in the ligand-bound conformations of the ECD (Sanders et al., 2013), and domain II has recently been identified as a potential mediator of subtle differences in ligand binding and specific receptor states (Bessman et al., 2014). Further, mutations in the JM-A region alter the energetics of ligand binding to the ECD (Macdonald-Obermann and Pike, 2009), and there is clear evidence that the active conformation of the EGFR TM is flexible and capable of adopting multiple conformation (Endres et al., 2013), like other single pass TM domains (Dominguez et al., 2014). Taken together, these observations support a model in which different ligand-dependent JM-A conformations result from three distinct ligand-bound ECD conformations that are transmitted faithfully through the membrane-sequestered TM helical dimer.

Our results support a recent theory that EGFR displays ligand functional selectivity (Wilson et al., 2009), or biased signaling, such that activation by a ligand stimulates the population of distinct conformations that singularly dictate downstream signaling differences (Kahsai et al., 2011; Liu et al., 2012). While many RTKs respond to multiple ligands and effect liganddependent signaling, a molecular link between the structure of the ligand-bound receptor and its distinct ligand-mediated cellular outcome has not been firmly established (Thomas et al., 2011). Here, we report direct evidence that different extracellular EGFR ligands induce distinct conformations of the intracellular JM-A region of the receptor. There are multiple mechanisms by which different JM conformations could dictate downstream

signaling. First, it is possible that proteins known to bind to the JM-A region and induce various signaling pathways, such as calmodulin (Martin-Nieto and Villalobo, 1998), Nck adaptor protein (Hake et al., 2008), G $\alpha$ <sub>S</sub> (Poppleton et al., 2000), PKC (Hunter et al., 1984), p38<sup>MAPK</sup> (Takishima et al., 1988), are preferentially recruited by one specific JM conformation. It is also possible that differential display of nuclear (Lin et al., 2001) and basolateral (Ryan et al., 2010) sorting motifs in the JM-A could differentially traffic the receptor. Lastly, specific JM-A conformations could directly bind to the surface of the asymmetric kinase dimer leading to further propagation of subtle conformational changes through the kinase domains and differential C-terminal tail phosphorylation (Wilson et al., 2009). It may be possible to generate EGFR mutants that assemble into one coiled coil or the other irrespective of growth factor treatment. These mutants will provide confirmation that both structures are capable of auto-phosphorylation and evaluate the role of each in downstream events. Our observation of distinct ligand-dependent JM-A conformations in surface receptors does not support the current belief that ligand-dependent downstream signaling differences result from differences in the pH-dependent ligand occupancy of endocytosed receptors as our experiments were conducted with endocytosis inhibited (Ebner and Derynck, 1991; French et al., 1995). Interestingly, the validity of this theory has also been questioned by others (Fortian and Sorkin, 2014) and it is possible that ligand-dependent effects on cell state arise from a more complicated mechanism. Further experiments are necessary to distinguish between these various theories.

## SIGNIFICANCE

Many common cancers are caused by aberrant activation of the epidermal growth factor receptor (EGFR). How EGFR is activated by growth factors to direct different signaling outcomes is not understood. While it was originally proposed that growth factor-dependent signaling differences arise from differential occupancy of the receptor during endocytosis, here we show that EGFR decodes growth factor identity by adopting discrete conformations in each ligand-activated state. We use a pro-fluorescent small molecule probe in combination with computational modeling to detect and characterize three distinct ligand-activated conformations. We further discover that these conformations track with the downstream signaling profiles for each ligand, providing evidence for growth factor functional selectivity by EGFR.

## EXPERIMENTAL PROCEDURES

### RosettaDock modeling of JM interfaces

RosettaDock (Rosetta 3.4) (Gray et al., 2003) was used for all docking calculations. We used the JM model described by Jura et al. (Jura et al., 2009i) as the input with each helix of the short coiled-coiled-like structure treated as one of the two docking partners. This structure was run first through the docking prepack algorithm (Rosetta 3.4) to optimize initial side chain positions. The initial, relative positions of the two helices were both randomized. Both the outer and inner-stages of the low-resolution step of the docking procedure were cycled 20 times and all possible side chain rotamers were incorporated into the algorithm for the high-resolution step. 25,000 output structures were created and were sorted based on overall RosettaDock energy score. The 1000 top-scoring structures were

then processed by the cluster application (Rosetta 3.4) where the total number of clusters was limited to 100 and a 1.4 Å RMSD cutoff was used. The resulting clusters were ranked on the basis of their Rosetta energy scores.

### ReAsH labeling assay

ReAsH labeling was accomplished as described previously (Scheck et al., 2012) with the following changes: 63,000 cells were used to seed the experiment, Disperse Blue was omitted from the ReAsH labeling step, a 1:2000 dilution of Alexa Fluor® 488 Goat Anti-Mouse IgG, IgA, IgM (H+L) Antibody (2 mg/mL) was used as the secondary antibody in the last step, and nuclei were labeled with 1.62 µM Hoechst 33342 for 5 min at 37 °C. Additionally, EGF, TGF, HB-EGF, and BC were used at a concentration of 100 ng/mL while ligands with a weaker affinity including AR, ER, and EPI were used at concentration of 2 µg/mL.

### TIRF microscopy

TIRF microscopy was conducted on a Leica microsystems AM TIRF MC DMI6000B fitted with an EM-CCD camera (Hamamatsu) with either the HCX PL APO 63×/1.47 or 100×/1.47 oil corrective objectives. A 12 V 100 W Halogen lamp was used for fluorescence application. In TIRF mode, EGFR labeled with Alexa Fluor® 488 was excited using the 488 nm laser and ReAsH was excited with the 561 nm laser while signals were processed in the QAD TIRF filtercube. Hoechst-stained nuclei were visualized in epifluorescence mode with the CFP filtercube. Images were analyzed as described previously (Scheck et al., 2012).

### Western blot analysis of EGFR autophosphorylation

CHO-K1 cells were maintained in Ham's F-12K (Kaighn's) Medium with 10% FBS at 37 °C with 5% CO<sub>2</sub>. 100 mm dishes were seeded with  $1.5 \times 10^6$  cells for 18 hours at which point the cells were transfected with either wt or Cys-Cys EGFR variants of EGFR with TransIT-CHO kit according to the manufacturer's instructions. After 8 hours, the cells were serum starved for another 18 hours and then harvested using non-enzymatic cell dissociation solution, washed with Dulbecco's Phosphate Buffered Saline (DPBS) and 500,000 cells were pipetted into wells of a 96-well plate. To each well was added a 200 µL aliquot of one of the following reagents and the incubation continued at 37 °C for 5 minutes: serum-free media, 100 ng/mL of EGF, TGF, HBEGF, or BC in serum-free media, or 2 µg/mL of AR, ER or EPI in serum-free media. Cells were then washed with serum-free media and lysed in 120 µL of 50 mM Tris, 150 mM NaCl, 1 mM EDTA, 1 mM NaF, 1% Triton X-100, pH 7.5 with protease and phosphatase inhibitors (1 tablet/10 mL) for 1 – 2 hours on ice. Lysate was then clarified at 14,000 rcf for 25 min at 4 °C. For Western blot analysis, lysates were run on a 10% polyacrylamide SDS-PAGE gel and transferred to PVDF membranes using an iBlot (Invitrogen). Membranes were blocked with 5% milk in TBS-T (50 mM Tris, 150 mM NaCl, 0.1% Tween, pH 7.4) for 1 – 3 hours followed by an 4 °C overnight incubation of either rabbit α-pY1173 or mouse α-FLAG primary antibodies. Blots were then washed with 5% milk in TBS-T and incubated with either α-rabbit or α-mouse HRP conjugate secondary antibodies for 1 hour at room temperature and then washed with TBS-T and visualized using Clarity™ Western ECL reagents

## Statistical Analysis

Comparisons within groups were made using ANOVA. Pairwise comparisons within groups were made using Bonferroni's post-test after finding a significant difference using ANOVA. P values are corrected using Bonferroni's method (Shaffer, 1995) so that the family-wise error rate is 0.05.

## Supplementary Material

Refer to Web version on PubMed Central for supplementary material.

## ACKNOWLEDGMENTS

The authors are grateful to the N.I.H. (GM 83257 to A.S. and F32 GM087092 to R.A.S) for support of this research. A.D. was supported by an NIH Training Grant in Biophysics (5T32GM008283-28).

## REFERENCES

- Adams S, Campbell R, Gross L, Martin B, Walkup G, Yao Y, Llopis J, Tsien R. New biarsenical Ligands and tetracysteine motifs for protein labeling in vitro and in vivo: Synthesis and biological applications. *J Am Chem Soc.* 2002; 124:6063–6076. [PubMed: 12022841]
- Arkhipov A, Shan Y, Das R, Endres NF, Eastwood MP, Wemmer DE, Kuriyan J, Shaw DE. Architecture and membrane interactions of the EGF receptor. *Cell.* 2013; 152:557–569. [PubMed: 23374350]
- Baldys A, Gooz M, Morinelli TA, Lee MH, Raymond JR, Luttrell LM, Raymond JR. Essential Role of c-Cbl in Amphiregulin-Induced Recycling and Signaling of the Endogenous Epidermal Growth Factor Receptor. *Biochemistry-US.* 2009; 48:1462–1473.
- Bessman, Nicholas J, Bagchi A, Ferguson, Kathryn M, Lemmon, Mark A. Complex Relationship between Ligand Binding and Dimerization in the Epidermal Growth Factor Receptor. *Cell Reports.* 2014; 9:1306–1317. [PubMed: 25453753]
- Burkhard P, Kammerer RA, Steinmetz MO, Bourenkov GP, Aebi U. The coiled-coil trigger site of the rod domain of cortexillin I unveils a distinct network of interhelical and intrahelical salt bridges. *Structure.* 2000; 8:223–230. [PubMed: 10745004]
- Croasdale R, Ivins FJ, Muskett F, Daviter T, Scott DJ, Hardy T, Smerdon SJ, Fry AM, Pfuhl M. An undecided coiled coil: the leucine zipper of Nek2 kinase exhibits atypical conformational exchange dynamics. *The Journal of biological chemistry.* 2011; 286:27537–27547. [PubMed: 21669869]
- Dominguez L, Foster L, Meredith SC, Straub JE, Thirumalai D. Structural heterogeneity in transmembrane amyloid precursor protein homodimer is a consequence of environmental selection. *J Am Chem Soc.* 2014; 136:9619–9626. [PubMed: 24926593]
- Ebner R, Derynck R. Epidermal Growth-Factor and Transforming Growth Factor- Alpha - Differential Intracellular Routing and Processing of Ligand-Receptor Complexes. *Cell Regul.* 1991; 2:599–612. [PubMed: 1777504]
- Endres NF, Das R, Smith AW, Arkhipov A, Kovacs E, Huang YJ, Pelton JG, Shan YB, Shaw DE, Wemmer DE, et al. Conformational Coupling across the Plasma Membrane in Activation of the EGF Receptor. *Cell.* 2013; 152:543–556. [PubMed: 23374349]
- Ferguson KM, Berger MB, Mendrola JM, Cho H-S, Leahy DJ, Lemmon MA. EGF activates its receptor by removing interactions that autoinhibit ectodomain dimerization. *Mol Cell.* 2003; 11:507–517. [PubMed: 12620237]
- Fortian A, Sorkin A. Live-cell fluorescence imaging reveals high stoichiometry of Grb2 binding to the EGF receptor sustained during endocytosis. *J Cell Sci.* 2014; 127:432–444. [PubMed: 24259669]
- French AR, Tadaki DK, Niyogi SK, Lauffenburger DA. Intracellular Trafficking of Epidermal Growth-Factor Family Ligands Is Directly Influenced by the Ph Sensitivity of the Receptor-Ligand Interaction. *Journal of Biological Chemistry.* 1995; 270:4334–4340. [PubMed: 7876195]

- Garrett TPJ, McKern NM, Lou MZ, Elleman TC, Adams TE, Lovrecz GO, Zhu HJ, Walker F, Frenkel MJ, Hoyne PA, et al. Crystal structure of a truncated epidermal growth factor receptor extracellular domain bound to transforming growth factor alpha. *Cell*. 2002; 110:763–773. [PubMed: 12297049]
- Goodman JL, Fried DB, Schepartz A. Bipartite Tetracysteine Display Requires Site Flexibility for ReAsH Coordination. *Chembiochem*. 2009; 10:1644–1647. [PubMed: 19533719]
- Gray JJ, Moughon S, Wang C, Schueler-Furman O, Kuhlman B, Rohl CA, Baker D. Protein-protein docking with simultaneous optimization of rigid-body displacement and side-chain conformations. *Journal of molecular biology*. 2003; 331:281–299. [PubMed: 12875852]
- Hake MJ, Choowongkamon K, Kostenko O, Carlin CR, Sonnichsen FD. Specificity determinants of a novel nck interaction with the juxtamembrane domain of the epidermal growth factor receptor. *Biochemistry-U.S.* 2008; 47:3096–3108.
- Hunter T, Ling N, Cooper JA. Protein Kinase-C Phosphorylation of the Egf Receptor at a Threonine Residue Close to the Cytoplasmic Face of the Plasma-Membrane. *Nature*. 1984; 311:480–483. [PubMed: 6090944]
- Jura N, Endres NF, Engel K, Deindl S, Das R, Lamers MH, Wemmer DE, Zhang XW, Kuriyan J. Mechanism for Activation of the EGF Receptor Catalytic Domain by the Juxtamembrane Segment. *Cell*. 2009a; 138:604–604.
- Jura N, Endres NF, Engel K, Deindl S, Das R, Lamers MH, Wemmer DE, Zhang XW, Kuriyan J. Mechanism for Activation of the EGF Receptor Catalytic Domain by the Juxtamembrane Segment (vol 137, pg 1293, 2009). *Cell*. 2009i; 138:604–604.
- Kahsai AW, Xiao KH, Rajagopal S, Ahn S, Shukla AK, Sun JP, Oas TG, Lefkowitz RJ. Multiple ligand-specific conformations of the beta(2)-adrenergic receptor. *Nat Chem Biol*. 2011; 7:692–700. [PubMed: 21857662]
- Lin SY, Makino K, Xia WY, Matin A, Wen Y, Kwong KY, Bourguignon L, Hung MC. Nuclear localization of EGF receptor and its potential new role as a transcription factor. *Nat Cell Biol*. 2001; 3:802–808. [PubMed: 11533659]
- Liu JJ, Horst R, Katritch V, Stevens RC, Wuthrich K. Biased Signaling Pathways in beta(2)-Adrenergic Receptor Characterized by F-19-NMR. *Science*. 2012; 335:1106–1110. [PubMed: 22267580]
- Lu C, Mi L-Z, Grey MJ, Zhu J, Graef E, Yokoyama S, Springer TA. Structural Evidence for Loose Linkage between Ligand Binding and Kinase Activation in the Epidermal Growth Factor Receptor. *Mol Cell Biol*. 2010; 30:5432–5443. [PubMed: 20837704]
- Luedtke NW, Dexter RJ, Fried DB, Schepartz A. Surveying polypeptide and protein domain conformation and association with FAsH and ReAsH. *Nat Chem Biol*. 2007; 3:779–784. [PubMed: 17982447]
- Macdonald-Obermann JL, Pike LJ. The Intracellular Juxtamembrane Domain of the Epidermal Growth Factor (EGF) Receptor Is Responsible for the Allosteric Regulation of EGF Binding. *J Biol Chem*. 2009; 284:13570–13576.
- Martin-Nieto J, Villalobo A. The human epidermal growth factor receptor contains a juxtamembrane calmodulin-binding site. *Biochemistry-U.S.* 1998; 37:227–236.
- Meier M, Stetefeld J, Burkhard P. The many types of interhelical ionic interactions in coiled coils - an overview. *Journal of structural biology*. 2010; 170:192–201. [PubMed: 20211731]
- Nygaard R, Zou YZ, Dror RO, Mildorf TJ, Arlow DH, Manglik A, Pan AC, Liu CW, Fung JJ, Bokoch MP, et al. The Dynamic Process of beta(2)-Adrenergic Receptor Activation. *Cell*. 2013; 152:532–542. [PubMed: 23374348]
- Ogiso H, Ishitani R, Nureki O, Fukai S, Yamanaka M, Kim J, Saito K, Sakamoto A, Inoue M, Shirouzu M, et al. Crystal structure of the complex of human epidermal growth factor and receptor extracellular domains. *Cell*. 2002; 110:775–787. [PubMed: 12297050]
- Poppleton HM, Sun H, Mullenix JB, Wiepz GJ, Bertics PJ, Patel TB. The juxtamembrane region of the epidermal growth factor receptor is required for phosphorylation of G alpha(s). *Arch Biochem Biophys*. 2000; 383:309–317. [PubMed: 11185568]

- Reddy CC, Wells A, Lauffenburger DA. Comparative mitogenic potencies of EGF and TGF alpha and their dependence on receptor-limitation versus ligand-limitation. *Med Biol Eng Comput.* 1998; 36:499–507. [PubMed: 10198537]
- Roepstorff K, Grandal MV, Henriksen L, Knudsen SLJ, Lerdrup M, Grovdal L, Willumsen BM, van Deurs B. Differential Effects of EGFR Ligands on Endocytic Sorting of the Receptor. *Traffic.* 2009; 10:1115–1127. [PubMed: 19531065]
- Ryan S, Verghese S, Cianciola NL, Cotton CU, Carlin CR. Autosomal Recessive Polycystic Kidney Disease Epithelial Cell Model Reveals Multiple Basolateral Epidermal Growth Factor Receptor Sorting Pathways. *Mol Biol Cell.* 2010; 21:2732–2745. [PubMed: 20519437]
- Saito T, Okada S, Ohshima K, Yamada E, Sato M, Uehara Y, Shimizu H, Pessin JE, Mori M. Differential activation of epidermal growth factor (EGF) receptor downstream signaling pathways by betacellulin and EGF. *Endocrinology.* 2004; 145:4232–4243. [PubMed: 15192046]
- Sanders JM, Wampole ME, Thakur ML, Wickstrom E. Molecular Determinants of Epidermal Growth Factor Binding: A Molecular Dynamics Study. *Plos One.* 2013:8.
- Scheck RA, Lowder MA, Appelbaum JS, Schepartz A. Bipartite Tetracysteine Display Reveals Allosteric Control of Ligand-Specific EGFR Activation. *ACS Chem Bio.* 2012; 7:1367–1376. [PubMed: 22667988]
- Scheck RA, Schepartz A. Surveying Protein Structure and Function Using Bis-Arsenical Small Molecules. *Accounts Chem Res.* 2011; 44:654–665.
- Seth D, Shaw K, Jazayeri J, Leedman PJ. Complex post transcriptional regulation of EGF-receptor expression by EGF and TGF-alpha in human prostate cancer cells. *Brit J Cancer.* 1999; 80:657–669. [PubMed: 10360641]
- Sinclair JK, Denton EV, Schepartz A. Inhibiting epidermal growth factor receptor at a distance. *J Am Chem Soc.* 2014; 136:11232–11235. [PubMed: 25075632]
- Takishima K, Friedman B, Fujiki H, Rosner MR. Thapsigargin, a Novel Promoter, Phosphorylates the Epidermal Growth-Factor Receptor at Threonine-669. *Biochem Bioph Res Co.* 1988; 157:740–746.
- Thomas C, Moraga I, Levin D, Krutzik PO, Podoplelova Y, Trejo A, Lee C, Yarden G, Vleck SE, Glenn JS, et al. Structural Linkage between Ligand Discrimination and Receptor Activation by Type I Interferons. *Cell.* 2011; 146:621–632. [PubMed: 21854986]
- Thoresen GH, Guren TK, Sandnes D, Peak M, Agius L, Christoffersen T. Response to transforming growth factor or (TGF alpha) and epidermal growth factor (EGF) in hepatocytes: Lower EGF receptor affinity of TGF alpha is associated with more sustained activation of p42/p44 mitogen-activated protein kinase and greater efficacy in stimulation of DNA synthesis. *J Cell Physiol.* 1998; 175:10–18. [PubMed: 9491776]
- Wilson KJ, Gilmore JL, Foley J, Lemmon MA, Riese DJ. Functional selectivity of EGF family peptide growth factors: Implications for cancer. *Pharmacol Therapeut.* 2009; 122:1–8.
- Wilson KJ, Mill C, Lambert S, Buchman J, Wilson TR, Hernandez-Gordillo V, Gallo RM, Ades LMC, Settleman J, Riese DJ. EGFR ligands exhibit functional differences in models of paracrine and autocrine signaling. *Growth Factors.* 2012; 30:107–116. [PubMed: 22260327]
- Zhang X, Gureasko J, Shen K, Cole PA, Kuriyan J. An allosteric mechanism for activation of the kinase domain of epidermal growth factor receptor. *Cell.* 2006; 125:1137–1149. [PubMed: 16777603]

**Highlights**

- Three distinct, ligand-activated JM coiled-coil conformations characterized.
- JM structure correlates growth factor identity with downstream signaling.
- A new mechanism by which EGFR could exhibit functional selectivity is proposed.
- Encoding growth factor identity in JM rotamers facilitates information transfer.



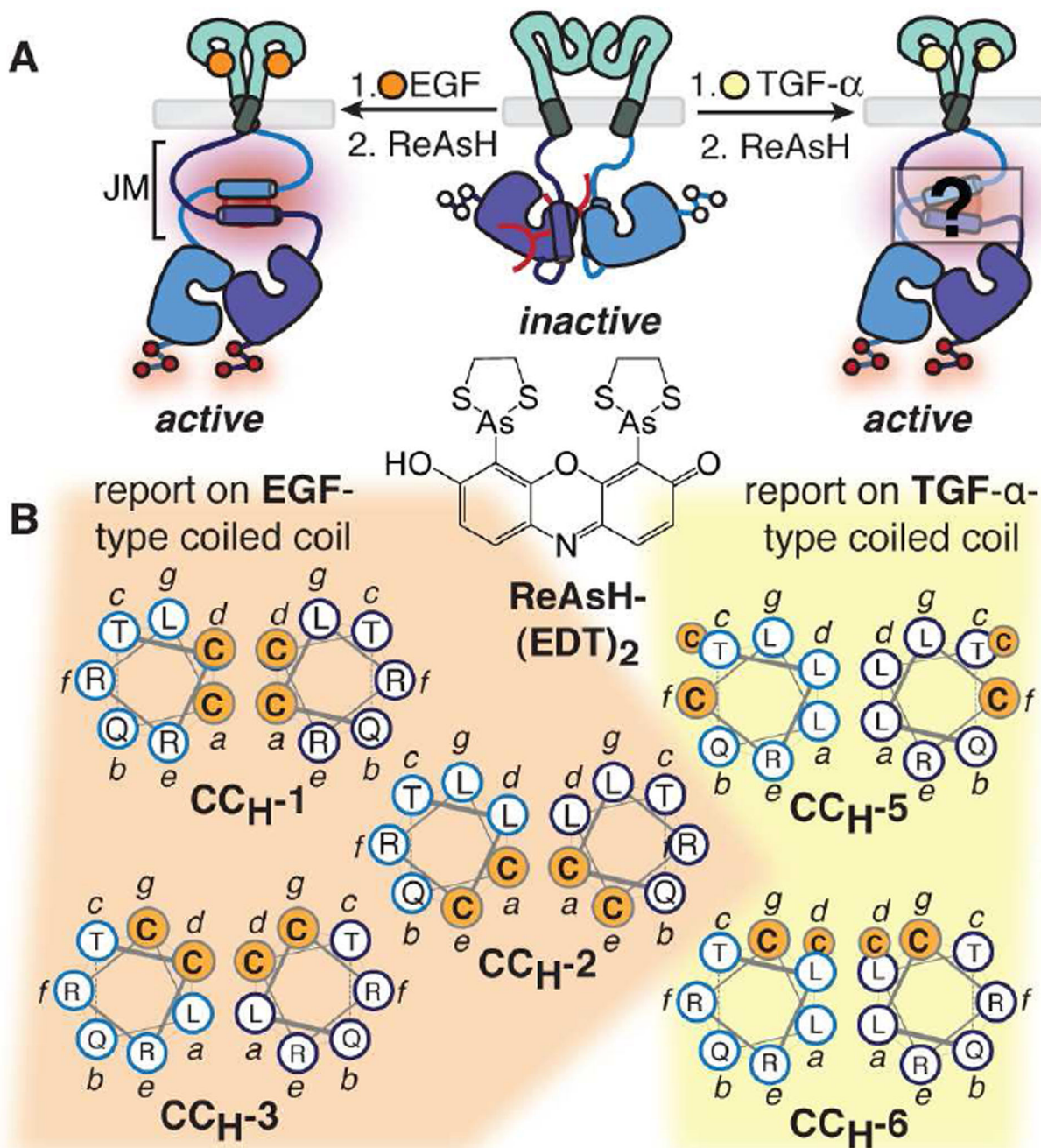


**Figure 1.**

Probing juxtamembrane segment (JM) structure within full length EGFR on the cell surface using bipartite tetracycysteine display (Luedtke et al., 2007; Scheck and Schepartz, 2011) and TIRF microscopy.

(A) EGF and TGF-α induce different structures within the EGFR JM (Luedtke et al., 2007; Scheck et al., 2012; Scheck and Schepartz, 2011).

(B) Helical wheel diagrams of five EGFR variants used previously to distinguish anti-parallel coiled coil arrangements. For sequences, see Figure S1A. In CC<sub>H</sub>-6, the Cys-Cys

motifs are separated axially by a helical turn and do not assemble a ReAsH binding site (see also Figure S1).

Author Manuscript

Author Manuscript

Author Manuscript

Author Manuscript

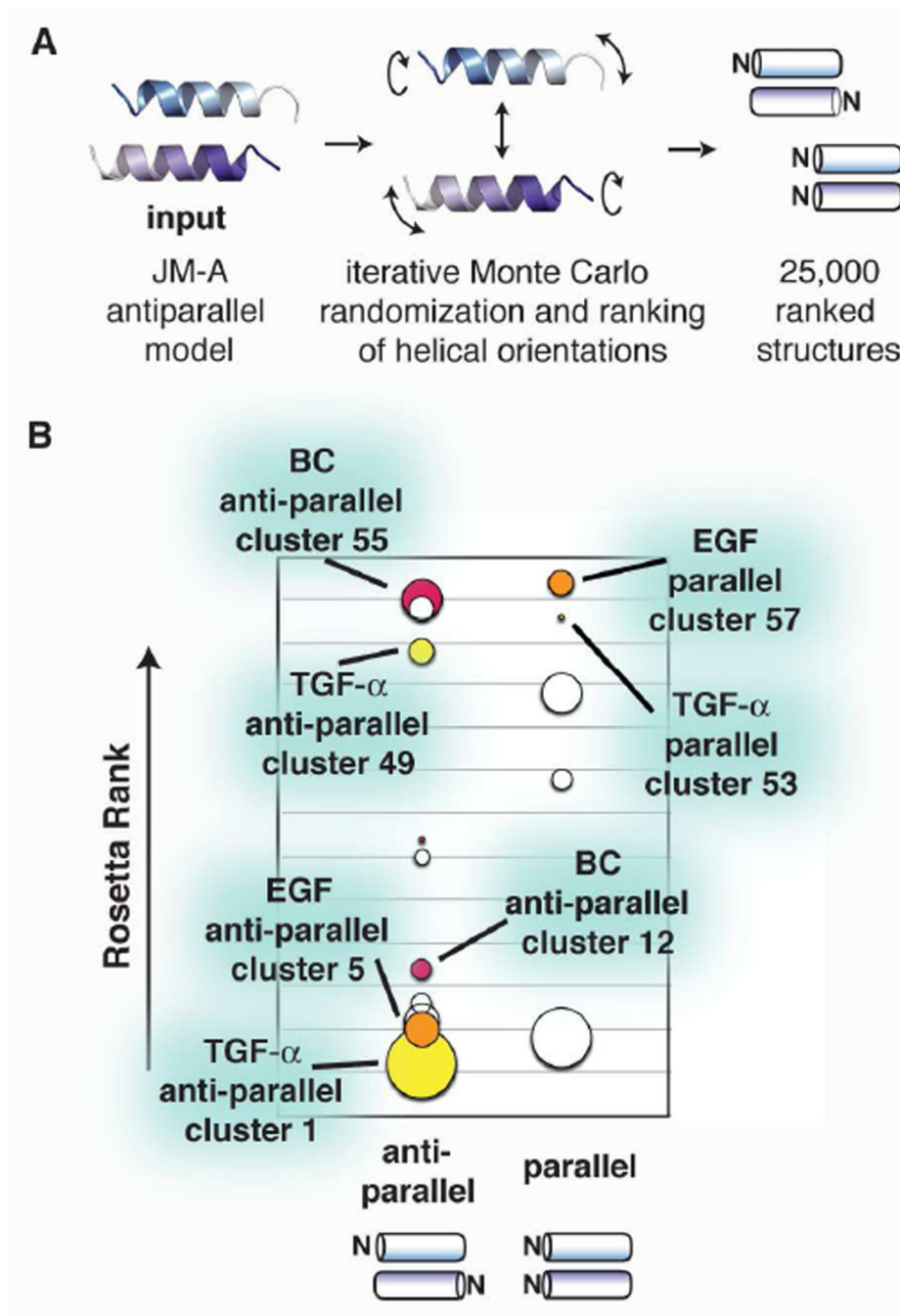


**Figure 2.** RosettaDock (Gray et al., 2003) analysis of the EGFR juxtamembrane segment (JM) conformational landscape.  
 (A) Procedure used to generate and evaluate potential paired helix interactions of the EGFR JM.  
 (B) Low energy structures identified by RosettaDock ranked in order of increasing Rosetta score and separated by strand orientation. Clusters representing possible EGF-, TGF- $\alpha$ -, and

BC-type structures are shown in orange, yellow, and pink, respectively. For the relative Rosetta rank of all clusters, see also Figure S2.

Author Manuscript

Author Manuscript

Author Manuscript

Author Manuscript

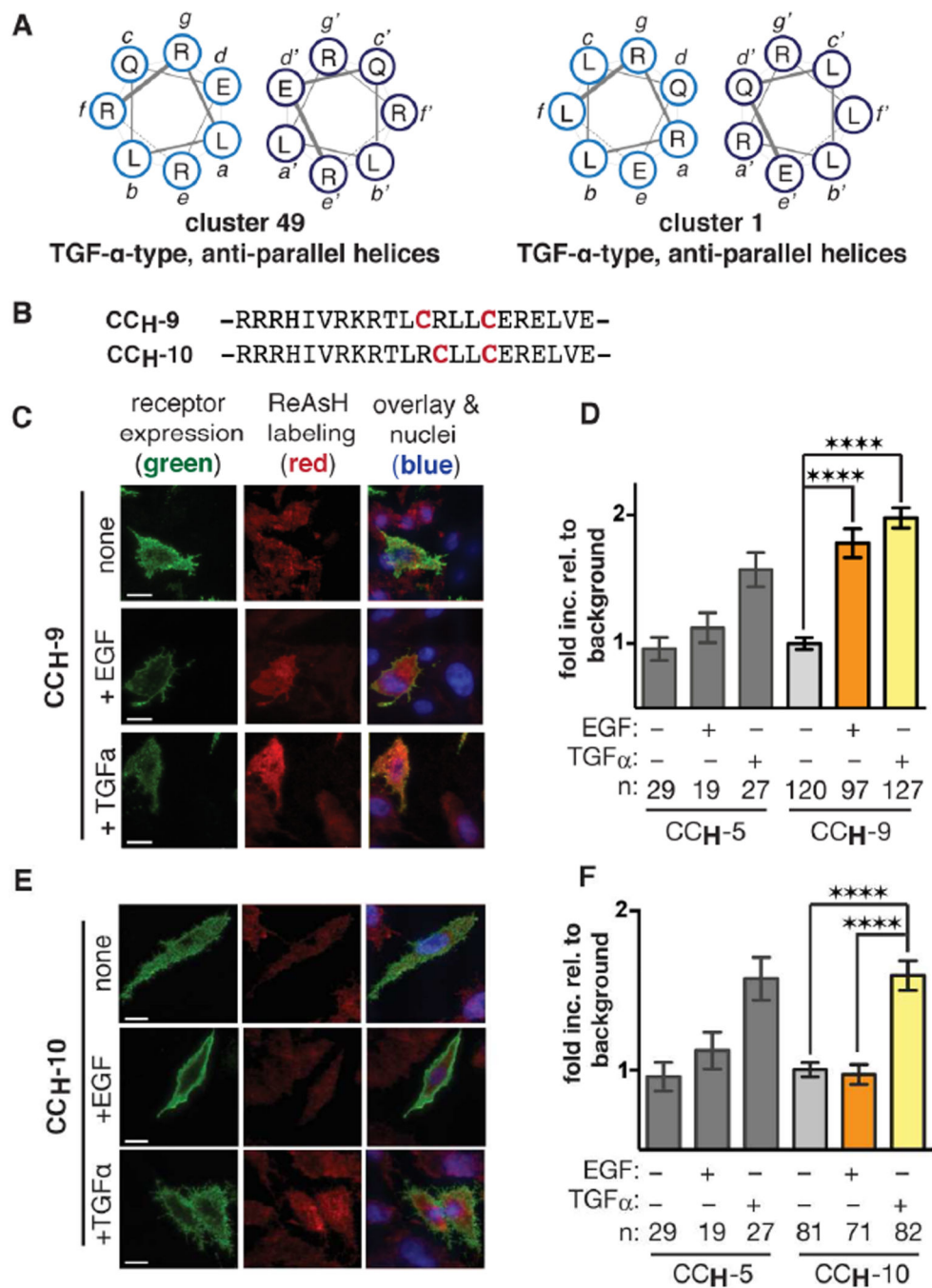


**Figure 3.**  
TGF- $\alpha$  induces an ‘inside-out’ helical interaction in the JM-A.  
(A) Helical wheel diagrams illustrating two anti-parallel interfaces potentially adopted in the presence of TGF- $\alpha$ .  
(B) JM-A regions of CC<sub>H</sub>-9 and CC<sub>H</sub>-10.  
(C,E) TIRF images of CHO-K1 cells expressing either FLAG-tagged CC<sub>H</sub>-9 or CC<sub>H</sub>-10 (green fluorescence) and treated with EGF or TGF- $\alpha$  (1 ng/mL) and ReAsH. Bars represent 10  $\mu$ m.

(D,F) Quantified fold increase in expression-corrected ReAsH fluorescence over background cells expressing CC<sub>H</sub>-9 or CC<sub>H</sub>-10 and treated with or without EGF or TGF- $\alpha$ . We attribute the slightly lower ReAsH fluorescence of CC<sub>H</sub>-10 to the lower activity of this mutant (see also Figure S4E). Error bars represent standard error. \*\*\*\*  $p < 0.0001$  from one way ANOVA with Bonferroni post-test (see also Figure S4).

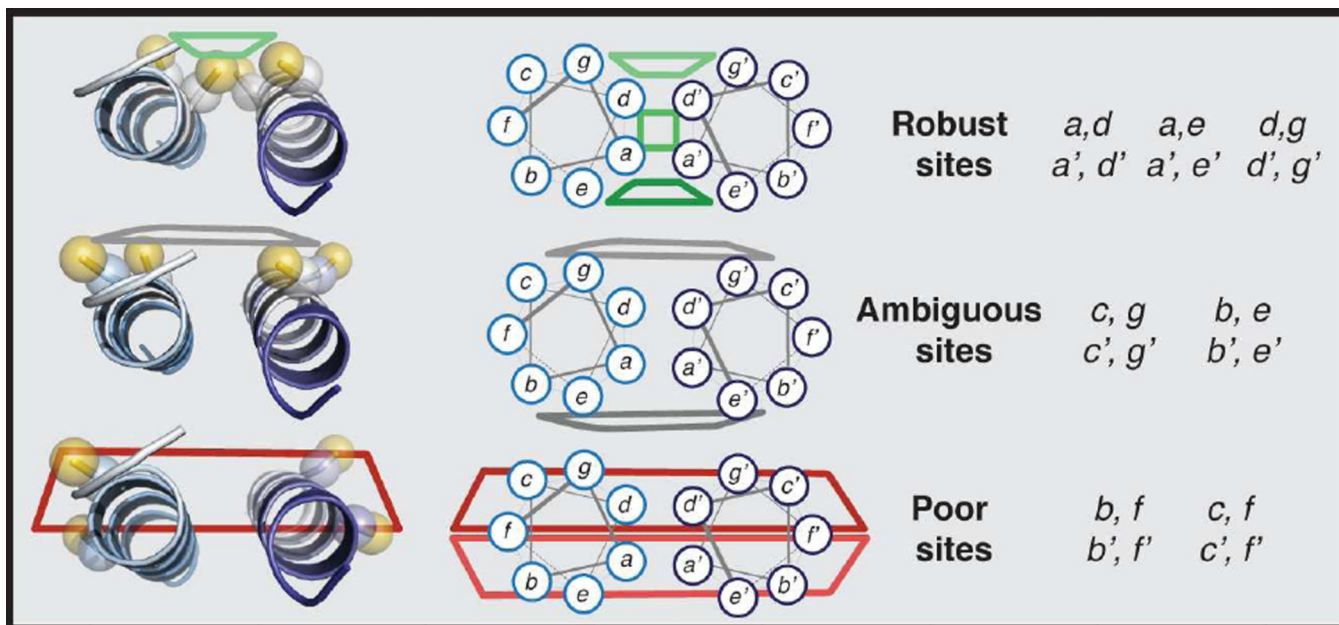
Author Manuscript

Author Manuscript

Author Manuscript

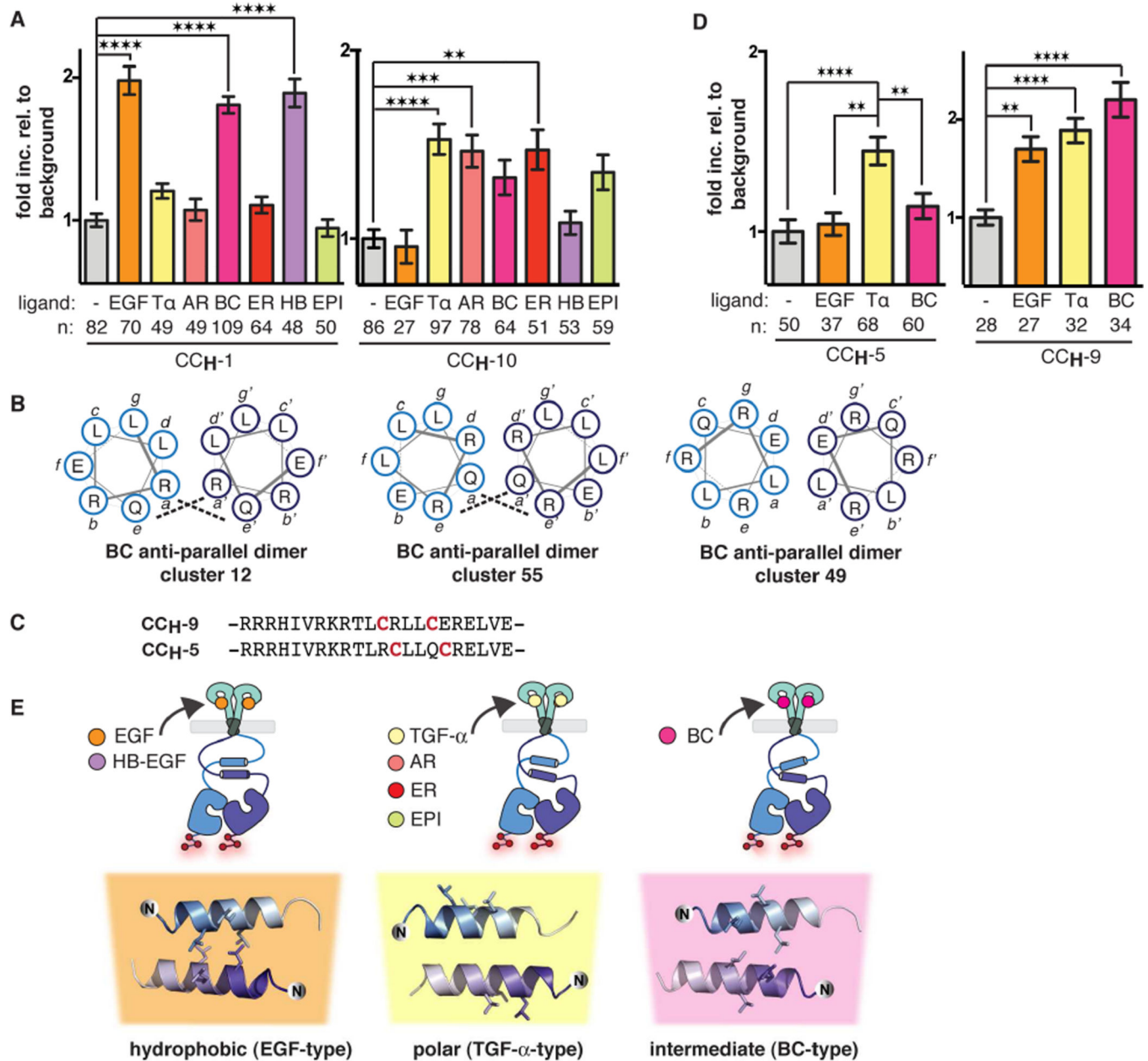
Author Manuscript





**Figure 4.** Categorization of three types of Cys-Cys ReAsH-binding sites formed by dimeric coiled coils as defined by cysteine proximity.



**Figure 5.**

JM-A conformation correlates with effects on downstream signaling.

(A) Quantified fold increase in expression-corrected ReAsH fluorescence over background of cells expressing CC<sub>H</sub>-1 or CC<sub>H</sub>-10 and treated with either EGF, TGF- $\alpha$ , BC, HB-EGF (1 ng/mL) or AR, ER, or EPI (2  $\mu$ g/mL). For TIRF microscopy images and Western blots showing the activity of CC<sub>H</sub>-1 and CC<sub>H</sub>-10 upon stimulation with each growth factor, see also Figures S5A and S5B.

(B) Helical wheel diagrams illustrating the interfaces of three antiparallel structures potentially adopted in the BC-activated JM-A region of EGFR.

(C) CC<sub>H</sub>-5 and CC<sub>H</sub>-9 primary sequences.

(D) Quantified fold increase in expression-corrected ReAsH fluorescence over background of cells expressing CC<sub>H</sub>-5 or CC<sub>H</sub>-9 and treated with or without EGF, TGF- $\alpha$ , or BC (1 ng/mL). For helical wheel diagrams showing the relative orientation of Cys-Cys motifs in EGFR variants when assembled into the anti-parallel coiled coils defined by clusters 12, 55, and 49, see Figures S5C and S5D. For TIRF microscopy images and Western blots showing the activity of CC<sub>H</sub>-5 and CC<sub>H</sub>-9 upon stimulation with EGF, TGF- $\alpha$ , and BC, see Figures S5F and S5G.

(E) EGFR stimulates three ligand-stimulated JM-A conformations. Activation by EGF and HBEGF is best represented by cluster 5 structures with a hydrophobic interface while activation by TGF- $\alpha$ , AR, ER, and EPI are best represented by cluster 1 structures with a polar interface. BC-activated EGFR likely adopts an intermediary conformation represented by cluster 12. All structures show the side chains of L655, L658, and L659 explicitly. Error bars represent standard error. \*\*  $p < 0.01$ , \*\*\*  $p < 0.001$ , \*\*\*\*  $p < 0.0001$  from one way ANOVA with Bonferroni post test (see also, Figure S5).